

Infant mortality in the hierarchical merging scenario: Dependency on gas expulsion timescales

R. Smith^{1*}, S. Goodwin², M. Fellhauer¹, P. Assmann¹

¹*Departamento de Astronomía, Universidad de Concepción, Casilla 160-C, Concepción, Chile*

²*Department of Physics and Astronomy, University of Sheffield, Hicks Building, Hounsfield Road, Sheffield, S3 7RH, UK*

Accepted to MNRAS, October 1st 2012

ABSTRACT

We examine the effects of gas expulsion on initially sub-structured and out-of-equilibrium star clusters. We perform N -body simulations of the evolution of star clusters in a static background potential before adjusting that potential to model gas expulsion. We investigate the impact of varying the rate at which the gas is removed, and the instant at which gas removal begins.

Reducing the rate at which the gas is expelled results in an increase in cluster survival. Quantitatively, this dependency is approximately in agreement with previous studies, despite their use of smooth, and virialised initial stellar distributions.

However, the instant at which gas expulsion occurs is found to have a strong effect on cluster response to gas removal. We find if gas expulsion occurs prior to one crossing time, cluster response is poorly described by *any* global parameters. Furthermore in real clusters the instant of gas expulsion is poorly constrained. Therefore our results emphasise the highly stochastic and variable response of star clusters to gas expulsion.

Key words: methods: numerical — methods: N -body simulations — stars: formation — galaxies: star clusters: general

1 INTRODUCTION

Many young stars are found in clusters. The fraction which are found in clusters depends on one's definition of a cluster (see Lada & Lada 2003; Bressert et al. 2010), and how exactly a cluster is defined (bound vs. unbound, see e.g. Gieles & Portegies Zwart 2011). However one looks at it though, star ‘clusters’ are clearly an important mode of star formation, if not the dominant mode.

Most stars appear to form in groups of tens to thousands of members embedded in molecular clouds. The initial distribution of stars follows the complex clumpy and filamentary structure of the underlying gas (see e.g. Kirk et al. 2007; Gutermuth et al. 2009; Peretto & Fuller 2009; Bressert et al. 2010; di Francesco et al. 2010; Maury et al. 2011). Simulations of initially smooth clouds of molecular gas, that are seeded with supersonic turbulence, fragment into filamentary structures (Bonnell et al. 2003; Bate & Bonnell 2004; Bate 2009; Girichidis et al. 2011). These structures may collapse to form stars if they become self-gravitating. It has been argued that clusters form as entities within this complex distribution (e.g. Marks & Kroupa 2011), or that they can form afterwards by mergers of stars and stellar groups from this complex distribution

(Allison et al. 2009; Allison et al. 2010). Clearly the initial dynamical state of the young stars will play a crucial role in forming bound clusters or unbound associations (Allison et al. 2009; Gieles & Portegies Zwart 2011).

In this paper we will take the view that clusters form within the hierarchical merging scenario (Allison et al. 2009; Allison et al. 2010) and, together with gas not used in star formation, they form bound objects. Observations show very few young clusters associated with natal gas older than ~ 5 Myr (Lada & Lada 2003; Lada 2010). It is assumed that feedback from massive stars removes residual gas in a gas expulsion phase. This gas expulsion will significantly alter the potential felt by the stars and can result in the destruction of the cluster (e.g. Tutukov 1978; Hills 1980; Goodwin & Bastian 2006; Baumgardt & Kroupa 2007; Goodwin 2009). This is often cited as the cause of ‘infant mortality’: the apparently high destruction rate of young clusters¹ (e.g. Lada & Lada 2003).

Previous work on gas expulsion has tended to concentrate on clusters in which the gas and stars are in virial and dynamical equilibrium (but see Verschueren & David 1989; Goodwin 2009). The assumption of virial and dynamical

* E-mail: rsmith@astro-udec.cl

¹ Although it should be noted that the importance of infant mortality depends on one’s definition of a cluster.

equilibrium for young clusters can be used to infer the initial cluster population and properties from present-day populations (e.g. Parmentier & Gilmore 2007; Baumgardt et al. 2008; Parmentier et al. 2008). However, the assumption of equilibrium initial conditions means that there is a one-to-one correlation between survivability and the initial conditions.

This paper is part of a series in which we examine gas expulsion in the context of the hierarchical merging scenario in which the initial distributions of the stars and gas are not in dynamical equilibrium. Specifically they have an initial distribution which will cause them to collapse and form a bound cluster within the gas potential (Allison et al. 2009; Allison et al. 2010; Smith et al. 2011a,b).

In this paper we present a simple numerical experiment examining the evolution of non-equilibrium small- N clusters within a smooth background potential which models the gas. Whilst this is clearly not realistic (at birth stars follow a gas distribution which is extremely complex, see above) we wish to examine the stochasticity which complex stellar distributions introduce. As we shall see, statistically identical non-equilibrium clusters can evolve in *very* different ways even in our very simple numerical experiments² and this stochasticity removes the simple correlation between initial conditions and survivability that is so often assumed.

In this paper we examine the N -body evolution of highly non-equilibrium star clusters in background potentials designed to model the residual gas in young star clusters. Here we adjust the background potential to model the effects of gas expulsion on different timescales, starting at different times. We describe our initial conditions in Section 2, our results in Section 3, and then discuss the potential consequences in Section 4 before drawing our conclusions in Section 5.

2 INITIAL CONDITIONS

In this paper we present a very simple numerical experiment: a clumpy distribution of equal-mass stars moving in a smooth (Plummer) background potential which is then removed to simulate gas expulsion. This experiment is *not* meant to accurately reflect reality, rather it is meant to concentrate on a new important variable: complex initial stellar distributions which can introduce (very significant) stochasticity to the problem of gas expulsion. As we will discuss in Section 4 we feel it emphasises some crucial physical parameters that would be important in any more sophisticated simulations and, most importantly, in reality.

We perform our N -body simulations using the NBODY6 code (Aarseth 2003). In our simulations there are two separate mass distributions which we wish to model: the stars and the background gas potential.

2.1 Initial distributions

In all cases we model the stellar distribution as $N = 1000$ particles with equal masses of $0.5M_{\odot}$ resulting in a total stel-

lar mass of $500M_{\odot}$. We choose equal-mass particles in order to avoid complex two-body interactions and mass segregation. Allison et al. (2009) and Allison et al. (2010) showed that both of these effects can be extremely important in the violent collapse of cool, clumpy regions. However we wish to avoid complicating our simulations with these effects as we are interested in the effects of gas expulsion.

We distribute the stars within a radius of 1.5 pc with a fractal distribution. We choose the fractal dimension D to be $D = 1.6$. The fractal is constructed using the box fractal method described in detail in Goodwin & Whitworth 2004 (see also Allison et al. 2010). A fractal with $D = 1.6$ corresponds to a highly clumpy initial distribution (see upper-left panel of Figure 2). It should be noted that clumpy fractal clusters can vary considerably in appearance depending on the random realisation used and their subsequent evolution can be highly stochastic (see Allison et al. 2010; Smith et al. 2011a). When investigating their response to varying gas expulsion time-scales, we therefore conduct a minimum of 5 realisations of any cluster.

The gas within the star-forming region is modelled as a background Plummer potential with a mass $M_g = 3450 M_{\odot}$ and scale-radius $r_g = 1.0$ pc. The crossing-time of the region is $t_{cr} \sim 1.3$ Myr.

We emphasise that the gas potential does not follow the initial stellar distribution, nor does it react to changes in the stellar distribution as it evolves (it is not live). These are obviously extreme simplifications but, as we will discuss later, we feel that we capture the essence of the basic physics using such a simple model.

We set the initial velocity dispersion of the stars relative to the total potential (gas & stars) with initial stellar virial ratios, Q_i , of 0.2 (sub-virial), or 0.5 (virialised). Note that a clumpy stellar distribution with $Q_i = 0.5$ is *not* initially in dynamical equilibrium. Thus the cluster will evolve significantly due to violent relaxation.

2.2 Star formation efficiency

The choice of the initial mass (M_g) and Plummer radius (r_g) of the (Plummer) gas potential sets the *true* star formation efficiency (SFE), i.e. initial fraction of gas that has been turned into stars. For a gas mass of $M_g = 3450 M_{\odot}$, and scale radius $r_g = 1.0$ pc, within 1.5 pc the enclosed gas mass is $2000 M_{\odot}$. The stars are distributed out to 1.5 pc, with a total stellar mass of $M_s = 500 M_{\odot}$. Thus within a radius of 1.5 pc the true SFE is 20 per cent.

We note that this is below the critical SFE for the survival of a bound core from an initially virialised star-gas distribution with instantaneous gas expulsion (~ 30 per cent, Goodwin & Bastian 2006; Baumgardt & Kroupa 2007), and at the lower bound for the survival of a bound core for adiabatic gas expulsion (Baumgardt & Kroupa 2007).

2.3 Gas expulsion

Although young star clusters form embedded within the molecular gas from which they formed, few star clusters over ~ 5 Myr old remain associated with their gas (Lada & Lada 2003; Proszkow & Adams 2009). This is likely as a result of a number of mechanisms including radiative feedback from

² And it is difficult to see how the addition of more realistic physics can make the problem less stochastic rather than more.

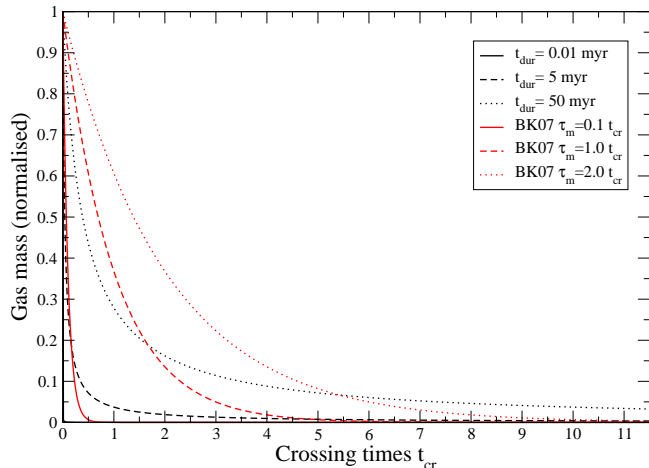


Figure 1. Plot of evolution of gas mass with time using Equation 1 (black curves), assuming $t_{\text{cr}}=1.3$ Myr. t_{dur} is the length of time required for the gas mass to be reduced to 99% of its initial value. When t_{dur} is short, gas loss occurs over a short duration. Our slowest gas mass-loss is when $t_{\text{dur}}=50$ Myr. For comparison, we include curves of the evolution of gas mass from Baumgardt & Kroupa (2007) (red curves). τ_m is the parameter from Baumgardt & Kroupa (2007) controlling the rate of gas loss. We see that $t_{\text{dur}}=50$ Myr results in similar gas mass-loss to when $\tau_m=1-2$ crossing-times.

massive stars, stellar winds from young stars, and eventually the first supernova(e). The time at which gas removal begins to occur, and the duration of the gas removal process is uncertain, and dependent on the particular gas removal mechanism in operation.

One of the main aims of our simulations is to examine the decoupling of the gas and stars *before* gas expulsion. If the gas and/or stars are not in equilibrium either as a whole, or with each other, then the relative distributions of the gas and stars will change. As shown in our previous papers (Smith et al. 2011a,b) if the stars can collapse relative to the gas distribution then the effect of gas expulsion is less important (see also Goodwin 2009 and references therein).

To simulate gas expulsion we parameterise the time evolution of the mass of the gas potential as:

$$M_g(t) = \frac{M_g(0)}{1 + \dot{M}(t - t_{\text{exp}})} \quad (1)$$

where t_{exp} is time at which gas expulsion begins, and \dot{M} controls the rate at which gas is removed.

We choose \dot{M} such that the gas mass $M_g(t)$ is reduced to 1 % of its initial value $M_g(0)$ over a specified duration time t_{dur} . For example, if $t_{\text{exp}} = 1$ Myr and $t_{\text{dur}} = 5$ Myr, then gas expulsion begins 1 Myr after the beginning of the simulation, and 99% the gas will be gone 5 Myr later.

We test the response of a cluster to four values when gas expulsion begins (t_{exp} : 0.1, 1, 5 & 9 Myr), and four values for how fast gas expulsion occurs (t_{dur} : 0.01, 1.0, 5.0 & 50.0 Myr). These timescales of gas expulsion cover the reasonable range of possible gas expulsion timescales from instantaneous to extremely slow (adiabatic) compared to

the crossing time. It is unclear what the typical gas expulsion timescales are, and they may depend on cluster mass (Kroupa & Boily 2002). For example, the relatively late supernovae of a low-mass O-star might result in a delayed start to gas expulsion.

In Figure 1, we illustrate the reduction in gas mass for gas expulsion that begins effectively immediately (t_{exp} : 0.1 Myr), and occurs over a duration t_{dur} : 0.01, 1.0, 5.0 & 50.0 Myr (black curves). We note that Baumgardt & Kroupa (2007) use an exponential form for the evolution of the gas mass that differs from ours in detail, but not in essence.

The Baumgardt & Kroupa (2007) form is shown on Figure 1 as red curves (labelled BK07). We see that our slowest gas mass reduction ($t_{\text{dur}}=50$ Myr) can be considered approximately equivalent to the gas mass loss in Baumgardt & Kroupa (2007) when $\tau_m=1-2$ crossing-times. We emphasise that while a 50 Myr duration (i.e. until 99 per cent gas loss) for gas expulsion may sound unrealistically lengthy, this is merely a result of the analytical form that we have used to model gas expulsion.

2.4 Cluster properties at time of gas expulsion

For a star-gas cluster which is initially smooth and in virial equilibrium (i.e. in dynamical equilibrium) and is no longer forming stars, its response to gas expulsion can be characterised by two parameters. Firstly, the true SFE, the relative gas mass to stellar mass (which does not change as the cluster is in equilibrium). Secondly, the timescale of gas expulsion from instantaneous (in less than a crossing time), to adiabatic (in several crossing times). See e.g. Baumgardt & Kroupa (2007).

However, Goodwin (2009) points out that the important variables are actually the virial state of the stars at the onset of gas expulsion and the timescale of gas expulsion. In an initially virialised cluster the virial state of the stars can be found directly from the true SFE. However if the cluster is not in equilibrium initially, then the virial state of the stars corresponds to an *effective* SFE which can be very different from the true SFE (see also Verschueren & David 1989; Goodwin & Bastian 2006).

In Smith et al. (2011a), we parameterise the effective SFE using two more physically meaningful quantities. The Local Stellar Fraction (LSF) is a measure of the mass of gas in the region where the stars are found (a form of evolving effective SFE). We also define the virial ratio of the stars at the moment of gas expulsion Q_{ge} .

The LSF is defined as

$$\text{LSF} = \frac{M_*(r < r_{\text{h}(s)})}{M_*(r < r_{\text{h}(s)}) + M_g(r < r_{\text{h}(s)})} \quad (2)$$

where $r_{\text{h}(s)}$ is the half-mass radius of the stars, and M_* and M_g are the mass of stars and gas, respectively.

The key aspects of the LSF and Q_{ge} are that they evolve with the dynamical evolution of the cluster. In Smith et al. (2011a) we found the LSF and Q_{ge} (measured when gas expulsion begins) to be effective predictors of the response of an initially out-of-equilibrium cluster to *instantaneous* gas expulsion after a few crossing times (in their case 2.5 initial crossing times).

We measure the survival of clusters to gas expulsion by

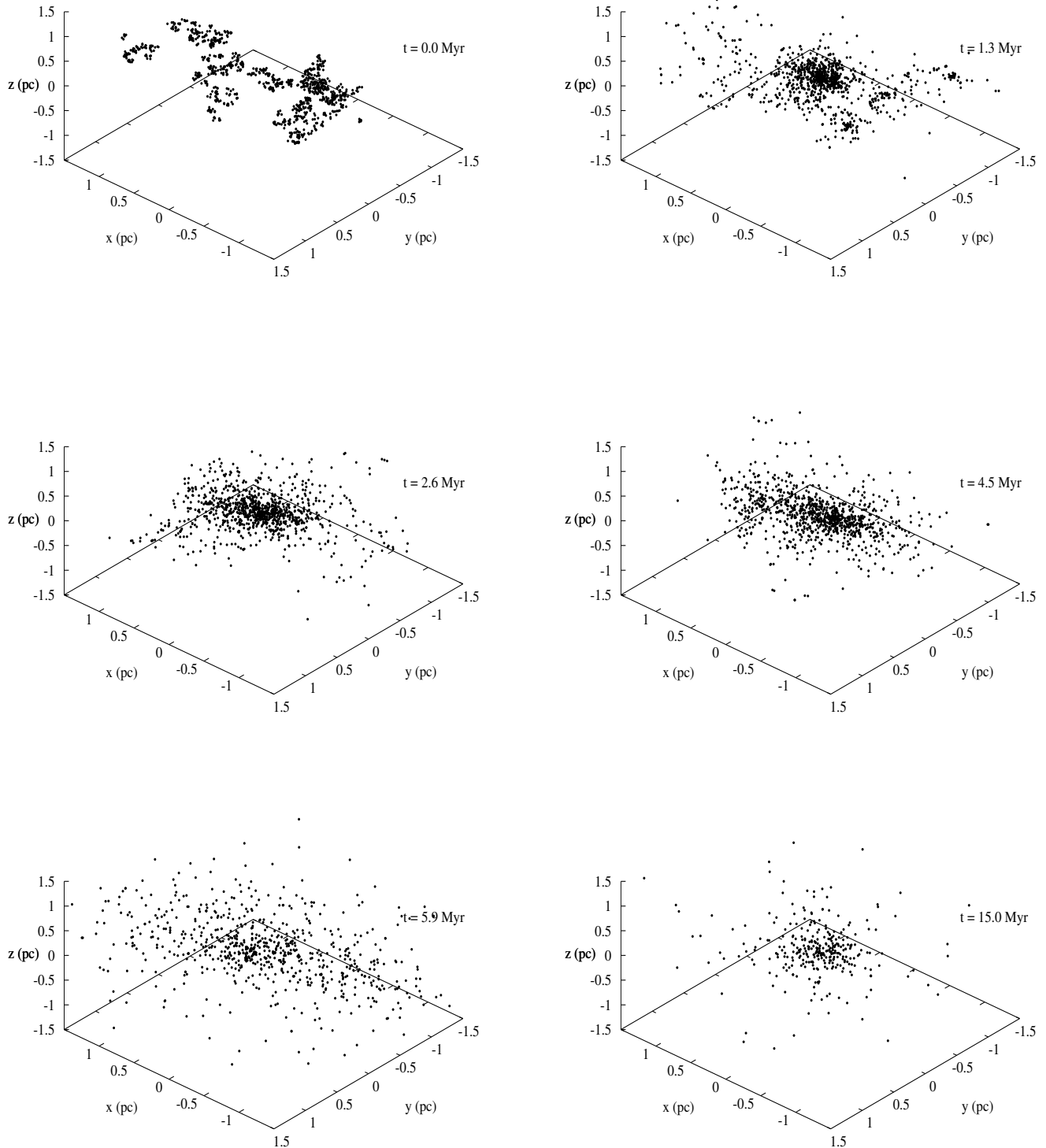


Figure 2. The evolution of an initially fractal ($D = 1.6$) stellar distribution in an $r_g = 1$ pc, $M_g = 3450M_\odot$ gas potential. The initial virial ratio of the stellar distribution within the gas background potential is $Q_i=0.2$. The time of each snapshot is indicated in the top-right hand corner of each panel. Initial clumpy substructure is erased with time. Instantaneous gas expulsion occurs at 5 Myr, resulting in unbound stars. By 15 Myr the final cluster is settled.

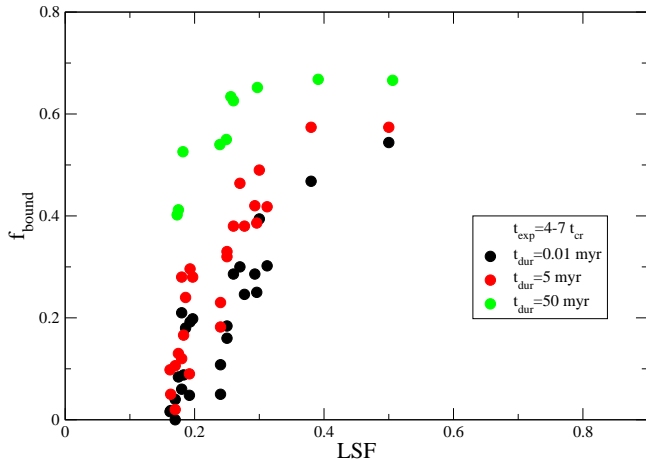


Figure 3. Final bound fraction of stars f_{bound} versus Local Stellar Fraction (LSF) for clusters where $t_{\text{exp}}=4-7 t_{\text{cr}}$. Symbol colour denotes the duration over which gas expulsion occurs (see legend). A trend for increasing f_{bound} with increasing LSF can be seen. If gas expulsion occurs more slowly, this trend shifts vertically upwards on the diagram. By eye, our slowest gas removal rate appears to result in an approximate increase in f_{bound} of ~ 0.3 .

measuring the fraction of stars that are bound to the cluster at $t = 15$ Myr. Where sub-structure remains following gas expulsion, we choose the most massive sub-clump to be the main cluster. We measure the number of stars that are bound to the cluster within the inertial frame of the cluster. This is because some clusters have a net velocity though simulation space following gas expulsion. To calculate the average velocity, we use only stars within a specific radius of the cluster centre. We vary the radius to ensure our final bound fraction is not sensitive to the radius we choose. When measuring the bound fraction we only include stars that are bound to the main cluster, and exclude stars that are bound to small subclumps in any remaining substructure.

2.5 Summary

We set-up clumpy $500M_{\odot}$ star clusters with $N = 1000$ equal-mass particles within a static background gas potential. The initial dynamical state of the stars varies from cool and subvirial ($Q_i=0.2$) to virialised ($Q_i=0.5$). We then allow the stars to dynamically evolve within the gas potential. Gas expulsion begins at a time $t = t_{\text{exp}}$. We vary t_{exp} from 0.1 Myr (essentially immediate gas expulsion) to 9 Myr (~ 7 crossing times). At the *start* of gas expulsion, we measure the Local Stellar Fraction of the cluster (LSF), and stellar virial ratio (Q_{ge}). We also vary the rate at which gas expulsion occurs by setting the parameter t_{dur} (the amount of time required for 99% of the gas to be expelled). We consider 4 values: $t_{\text{dur}} = 0.01, 1.0, 5.0, \& 50$ Myr. We measure the final bound fraction of each star cluster at $t = 15$ Myr to determine how well the cluster survives.

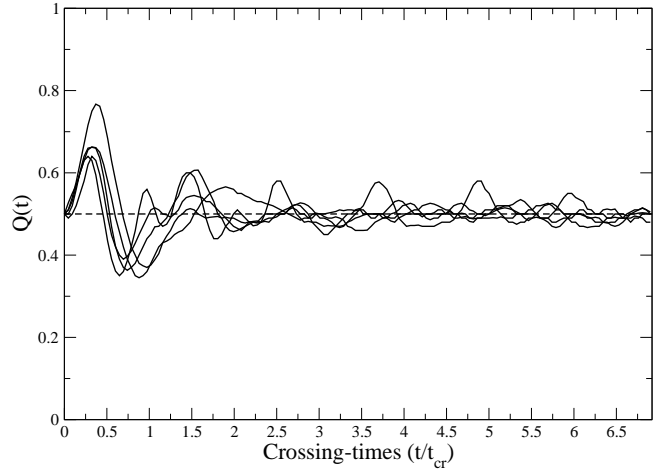


Figure 4. Evolution of the stellar virial ratio of 5 different fractal clusters. All start with a total virial ratio of $Q_i = 0.5$.

3 RESULTS

3.1 A representative example

We will first present a representative example, before focussing on the impact of the gas expulsion times scales. In Figure 2 we present an example of the evolution of an initially fractal $D = 1.6$ stellar distribution with an initial virial ratio of $Q_i = 0.2$ in the gas potential. The true SFE of this system is $\epsilon = 0.2$. In this particular example gas expulsion begins at 5 Myr, and then the gas is removed effectively instantaneously. The crossing-time of the region is ~ 1.3 Myr.

Figure 2 shows that the stellar component collapses and relaxes during the first two crossing times. The initial fractal distribution (first panel) is partly erased by one crossing time (second panel) and by two crossing times (third panel) the bulk of the cluster has collapsed into a dense core (cf. Allison et al. 2009; Smith et al. 2011a,b). At the onset of gas expulsion at 4.5 Myr (fourth panel) the stellar distribution is relatively relaxed with a halo of stars, mostly ejected by two-body interactions within the dense main stellar cluster. The effect of gas expulsion is as expected in that a significant fraction of stars are lost. At 5.9 Myr (fifth panel) many of these escaping stars are still associated with the cluster, but by 15 Myr (last panel) only a virialised bound core of stars remains.

The cool, clumpy initial distribution of the stars in this simulation cause them to collapse towards the centre of the gas potential. This causes the stars to virialise (i.e. Q_{ge} to approach 0.5), but it also causes the LSF to increase significantly as the stars are concentrated in the centre of the gas potential. For example, in Figure 2 the initial distribution of stars has an LSF=0.24 (close to the true SFE), but the final LSF at the time of gas expulsion has increased to 0.41.

3.2 Effects of varying the rate of gas expulsion

In all simulations, we evolve our stellar initial conditions in the gas potential until gas expulsion begins. At the start of gas expulsion we measure the LSF (see Equation 2) and the virial ratio Q_{ge} .

We simulate the evolution of 10 different realisations. For each ensemble we model gas expulsion occurring at $t_{\text{exp}} = 0.1, 1.0, 5.0 \& 9.0$ Myr. For each chosen t_{exp} , we model four durations over which the gas is expelled: $t_{\text{dur}} = 0.01, 1.0,$

5.0, & 50 Myr. We use $Q_i=0.2$ and 0.5. In total, we conduct 90 simulations. All simulations are conducted for 15 Myr in total (~ 11.5 initial crossing-times), when the final bound fraction f_{bound} of the cluster is measured.

The results of the $t_{\text{exp}}=5.0-9.0$ Myr ($t_{\text{exp}}=4-7$ crossing-times) simulations are shown on Figure 3 (we turn later to the effects of different t_{exp}). We plot the final bound fraction f_{bound} of the cluster against the LSF at the start of gas expulsion. The colour of the filled circle symbols denotes the duration over which their gas was removed. For clarity in Figure 3, we exclude the $t_{\text{dur}} = 1$ Myr points, this gas removal timescale is effectively instantaneous and the results are indistinguishable from the $t_{\text{dur}} = 0.01$ Myr points. Black symbols have almost instantaneous gas expulsion ($t_{\text{dur}}=0.01$ Myr). Red symbols lose their gas marginally more slowly ($t_{\text{dur}}=5$ Myr), and green symbols lose their gas the most slowly of all ($t_{\text{dur}}=50$ Myr). (For reference see Fig. 1.)

A trend can be seen in the relation between f_{bound} and the LSF in Figure 3. Firstly, as expected, lower LSFs tend to result in lower bound fractions. Also, as expected, slower gas removal (tending to adiabatic) tends to result in higher bound fractions (cf. Baumgardt & Kroupa 2007).

However, for low-LSFs there is a wide spread in the final bound fractions. For LSFs of ~ 0.2 (similar to the initial, true, SFE), the bound fractions vary between zero and over half. The largest bound fractions (all > 0.4) occur for adiabatic gas loss which is far less destructive (see above), but for an intermediate gas loss timescale of 5 Myr the spread is between zero and 0.3. We will return to this in the next section.

We do find broad agreement with the results of Baumgardt & Kroupa (2007) once the differences in our parameterisation of the gas expulsion timescale and our use of the LSF rather than true SFE are taken into account. Our LSF values are typically between 0.2 and 0.4. We therefore compare with the Baumgardt & Kroupa (2007) results for true SFEs in the same range. The upper-left panel of Figure 2 of Baumgardt & Kroupa (2007) shows that their bound fraction also increases by 20-40 per cent between their effectively instantaneous and their adiabatic gas expulsion timescales. Inspection of Figure 3 shows a similar relationship, albeit with *much* more scatter.

3.3 The evolution of the dynamical state of the stars

The scatter we find in the LSF- f_{bound} relationship for a given gas expulsion onset and duration comes from two sources. It is due to differences in the dynamical state of the stars at the onset of gas expulsion which, in turn, is due to the stochastic evolution of the initially non-equilibrium stellar distribution.

Figure 4 shows the evolution of the *stellar* virial ratios for 5 different fractals that initially have a total virial ratio of $Q_i = 0.5$. The stellar virial ratio is the virial ratio of the stars alone. We note that the potential of any individual star has a component from surrounding stars and another component from the surrounding gas potential. Both components are included in the virial ratio calculation.

Although the systems are initially in virial equilibrium, the fractal initial conditions mean that they are *not* in dy-

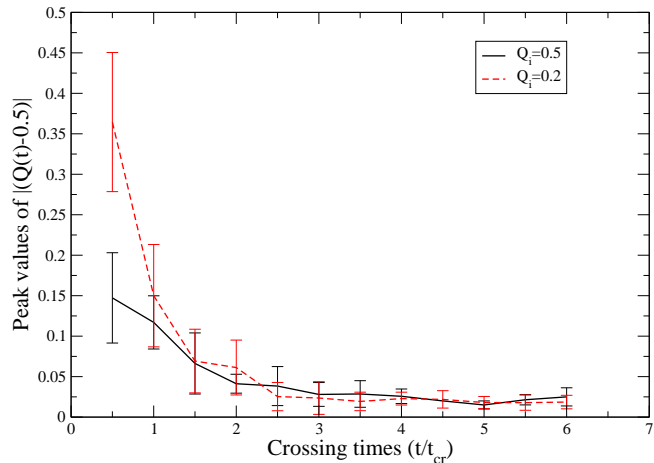


Figure 5. Evolution of peak values of $|(Q(t) - 0.5)|$ for 10 different initially virialised ($Q_i=0.5$) fractals and 10 different cool ($Q_i=0.2$) fractals. The average (and standard deviation) of the peak values are binned into half crossing-time bins. Peak values are initially larger, then reduce in size as the clusters attempt to virialise. Initially $Q_i=0.2$ fractals have larger deviations from virialised. After ~ 1.5 crossing-times, Q -evolution of $Q_i=0.2$ & 0.5 are similar. After 4-5 crossing-times, fractals have settled to close to virialised.

namical equilibrium. The stellar distributions violently relax and collapse which initially increases the stellar virial ratio before finding a roughly smooth, dense new configuration in the centre of the gas potential (with a correspondingly higher LSF). The stars then ‘bounce’, oscillating around virial equilibrium for several crossing times whilst they relax.

Smith et al. (2011a) found that the stellar virial ratio at the onset of gas expulsion is important to the cluster’s response to gas expulsion (see also Goodwin 2009). If the stellar virial ratio is slightly super-virial ($Q_{\text{ge}} > 0.5$), then the cluster will lose more stars (lower f_{bound}), whilst if they are slightly sub-virial ($Q_{\text{ge}} < 0.5$), then the cluster will retain more stars (higher f_{bound}). However, Smith et al. (2011a) only examined instantaneous gas expulsion after 2.5 crossing times.

To investigate the effects of Q_{ge} with different starting times and durations of gas expulsion we record the peak values of the deviation of the stellar distribution from virial equilibrium ($|(Q - 0.5)|$) and the time at which these maximum deviations occur. We conduct this test both for 10 different clusters that are initially globally virialised ($Q_i=0.5$), and 10 different clusters that are initially globally cool ($Q_i=0.2$). We calculate the mean and standard deviation of the peak values of $|(Q - 0.5)|$ in bins of half an initial crossing-time. The results are presented in Figure 5.

Figure 5 quantifies what is visible in Figure 4. Deviations from virialised are greater at early times as the stellar component relaxes. They are also greater in initially globally cool clusters ($Q_i=0.2$) as they have to relax more to reach (rough) equilibrium.

We can predict that the stellar virial ratio will be an important factor in that it will vary more, and be more stochastic, at early times. Firstly, the further clusters start away from equilibrium (dynamical or virial), the greater the initial variations can be. Secondly, the shorter the amount of time clusters have had to relax, the greater the variations can be.

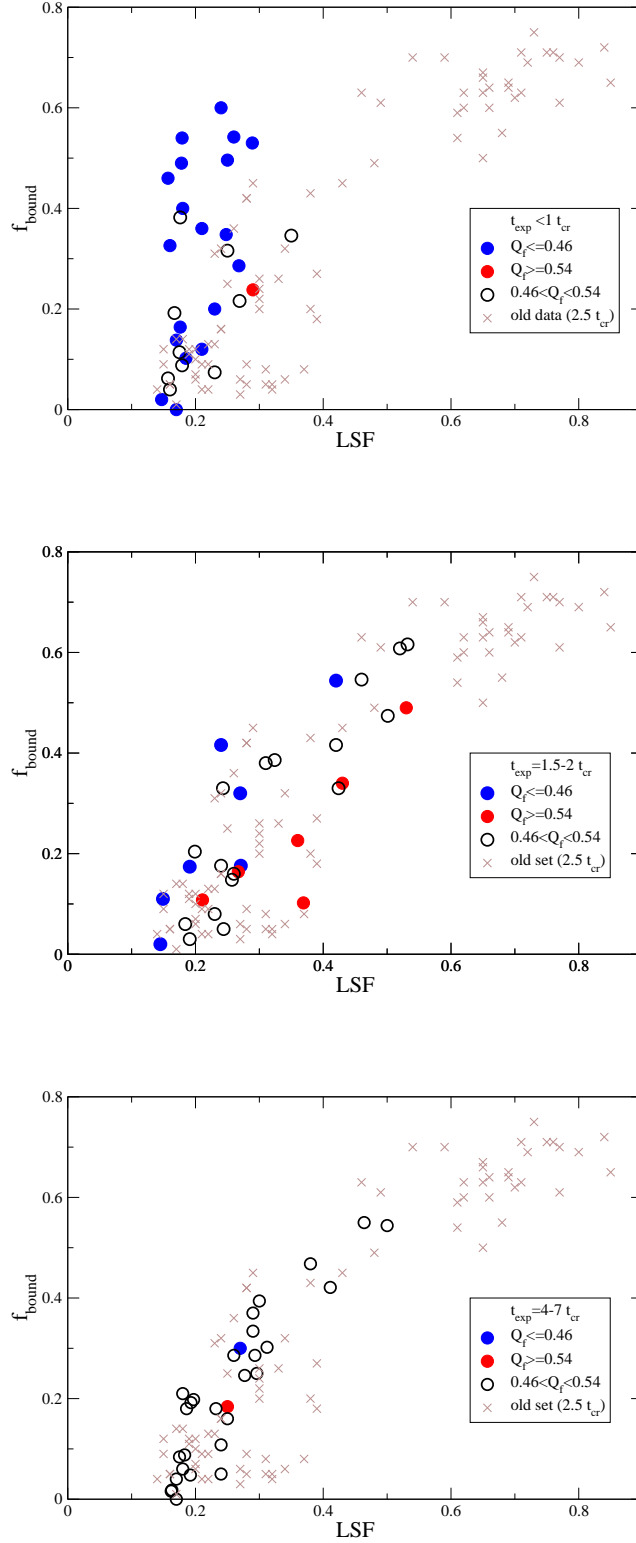


Figure 6. Final bound fraction of stars f_{bound} versus Local Stellar Fraction (LSF) for clusters with early gas removal ($t_{\text{exp}} < 1 t_{\text{cr}}$, upper panel), intermediate gas removal time ($t_{\text{exp}} = 1.5-2.0 t_{\text{cr}}$, middle panel), and late gas removal ($t_{\text{exp}} = 4-7 t_{\text{cr}}$, lower panel). In these models, when gas expulsion begins, it is effectively instantaneous ($t_{\text{dur}} = 0.01$ Myr). Clusters with $Q_i = 0.2$ result in lower LSF values, whereas $Q_i = 0.2$ clusters result in higher LSF values. The stellar virial ratio at the onset of gas expulsion Q_{ge} is either low (blue circles, $Q_{\text{ge}} < 0.46$), roughly virialised (open circles, $0.46 < Q_{\text{ge}} < 0.54$), or high (red squares, $Q_{\text{ge}} > 0.54$). Light crosses show the results from Smith et al. (2011a) for instantaneous gas expulsion at $t_{\text{exp}} = 2.5 t_{\text{cr}}$ for reference.

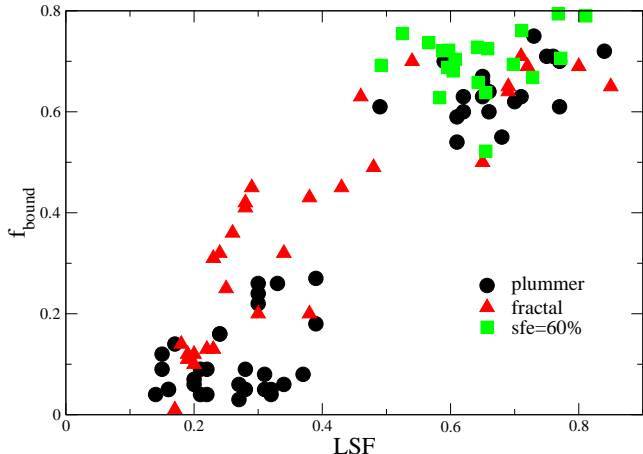


Figure 7. Final bound fraction of stars f_{bound} versus Local Stellar Fraction (LSF) for clusters with instantaneous gas expulsion at $t_{\text{exp}} = 2.5 t_{\text{cr}}$. Results from Smith et al. (2011a) where the star formation efficiency is 20%, and using an initial distribution of stars that is ‘Plummer-like’ (black circles), and fractal (red triangles). New results are shown for clusters with matching properties to the fractals (red triangles), but a much higher star formation efficiency of 60% (green squares). The scatter in the bound fraction is not highly sensitive to the form of the initial clumpy stellar morphology we choose, nor to the star formation efficiency.

3.4 The survival of clusters

From the above results and discussions we can see that the response of a cluster to gas expulsion, and the possible survival of a bound core as a remnant cluster, depend on several factors.

The relative importance of the gas potential to the stars (as measured by the LSF) is clearly very important. This, however, depends on the way in which the stellar distribution has relaxed relative to the gas and depends on the initial distribution (in this case highly clumpy) and initial velocity dispersion (measured by the total initial virial ratio Q_i) of the stars. It also depends on the exact dynamical state of the stars at the moment when gas expulsion occurs (Q_{ge}). And both the LSF and Q_{ge} depends to some extent on the stochastic details of the relaxation of each particular realisation (see Allison et al. 2010). The reaction of the cluster to gas expulsion also depends on the timescale of gas expulsion, with long (adiabatic) timescales being much less destructive.

In addition, as we will explore in this section, both the LSF and especially Q_{ge} evolve rapidly, especially in the first 1 – 2 crossing-times and so the effect of gas expulsion will depend strongly on the time of the onset of gas expulsion.

We have already investigated the effect of varying the rate of gas expulsion in Section 3.2. We now focus on the effect of varying the instant at which gas expulsion occurs, and fix the rate of gas expulsion to be effectively instantaneous.

Figure 6 shows the LSF- f_{bound} relationships for early gas expulsion (top panel, $t_{\text{exp}} < 1 t_{\text{cr}}$), intermediate gas expulsion (middle panel, $t_{\text{exp}} = 1.5 - 2.0 t_{\text{cr}}$), and late gas expulsion (bottom panel, $t_{\text{exp}} = 4 - 7 t_{\text{cr}}$). For all data points shown, when gas expulsion begins, the gas is removed instantaneously. Plotted on each panel in light crosses are the results from Smith et al. (2011a) instantaneous gas expul-

sion at $t_{\text{exp}} = 2.5 t_{\text{cr}}$ for reference. We combine the results for $Q_i=0.5$ and $Q_i=0.2$ star clusters in Figure 6.

The points marked with blue filled circles have a low stellar virial ratio at the moment of the onset of gas expulsion ($Q_{\text{ge}} < 0.46$), open circles are roughly virialised ($0.46 < Q_{\text{ge}} < 0.54$), and red squares are super-virial ($Q_{\text{ge}} > 0.54$).

The top panel shows the results for the early onset of gas expulsion. Early gas expulsion results in gas expulsion occurring whilst the stars are still relaxing. They tend to have a low virial ratio ($Q_{\text{ge}} < 0.46$) as they are still collapsing into a new equilibrium, and their LSF tends to be low (close to the true SFE) as they are still fairly widely distributed in the gas potential. The huge scatter in this top panel is due to the highly stochastic nature of the early dynamics of the clusters. Many of these clusters will still contain subclumps (see Figure 2) and the bulk dynamics of these subclumps is important. At these stages Q_{ge} is not a good indicator of survival as much of the stellar kinetic energy can be contained in bound clumps. If these clumps escape due to gas expulsion f_{bound} will be low (or even zero), however retaining one or two subclumps can result in a very high f_{bound} . Clumps also raise the stellar-to-gas fraction very locally at their centres. The LSF is insensitive to this as it measures the stellar-to-gas fraction on scales that are typically much larger than individual clumps (i.e. the half-mass radius of the stars).

For intermediate gas expulsion timescales (middle panel) the LSF becomes more important as the clusters tend to have had the time to relax into a smooth central cluster. More clusters are roughly virialised and there is a trend of f_{bound} decreasing with lower LSF as would be expected. As clusters are oscillating around virial equilibrium within the gas potential, the spread in f_{bound} for a given LSF is wide. At a fixed LSF, sub-virial clusters tend to higher f_{bound} than super-virial clusters. Therefore at intermediate gas expulsion timescales, a combination of Q_{ge} and LSF determine the response to gas expulsion.

For long gas expulsion timescales (bottom panel) the clusters have had a chance to virialise within the gas potential and so the relationship between the LSF and f_{bound} becomes much tighter with the LSF being the key factor in determining the response to gas expulsion.

3.5 Dependency on initial stellar morphology and star formation efficiency

First, we wish to test how sensitive our results are to the mathematical form of the initial clumpy distribution of stars we have chosen. To do this, we use models from Smith et al. (2011a) where we considered two types of clumpy distributions (or stellar morphologies) for the initial positions of our stars; fractal (like those modelled in this paper), and ‘Plummer-like’. In the ‘Plummer-like’ distribution there are 16 clumps of stars in total, and each clump is modelled as an individual Plummer sphere of mass $\sim 30 M_{\odot}$, and Plummer scale-length ~ 0.05 pc. The clumps themselves are distributed according to a Plummer distribution with a Plummer scale-length of 1-1.5 pc). Further details can be found in Smith et al. (2011a).

In Figure 7 we show the final bound fraction of stars f_{bound} versus Local Stellar Fraction (LSF) for clusters from

Smith et al. (2011a), but split into ‘Plummer-like’ (black circles), and fractal (red triangles). We recall that both groups have equal star formation efficiency of 20%, and both undergo instantaneous gas expulsion after 2.5 crossing-times - they differ only in their initial stellar morphology. We find that the trend, and its scatter in bound fraction, is not highly sensitive to which form of clumpy stellar morphology we choose. Two apparently separated groups of Plummer-like models are seen at high and low LSF. However this is mainly just a result of low numbers of Plummer-like models with $Q_i = 0.2-0.4$, whose presence would fill the gap between the two groups.

Secondly, we wish to test if our results differ when we consider clusters whose mass is dominated by stars, as we have so far only considered clusters that are heavily dominated by gas. Therefore we model 20 clusters with a much higher star formation efficiency of 60% (green squares). These differ from the fractals on Figure 7 in their star formation efficiency only. As expected, these clusters fall in the high LSF range. More importantly, we find that there is still a similar amount of scatter at higher star formation efficiency - despite the fact that the stars now dominate the mass of the cluster. In fact, the virial state at the time of gas expulsion Q_{ge} continues to play the same role, broadening the trend, as when the star formation efficiency was 20%.

In summary, the trend and its scatter is not very sensitive to the form of the initial clumpy stellar morphology we choose, nor to the star formation efficiency (i.e. the strength of the rigid background potential).

4 DISCUSSION

We have examined the response of young clusters to gas expulsion as measured by their ability to retain a bound core of stars and avoid complete destruction: their survivability.

Clusters older than ~ 5 Myr are not seen to be associated with the gas from which they formed. There are two possibilities for the fate of this gas. Firstly, that all of the gas was used in star formation (100 per cent efficiency). However this is unlikely as shortly after a massive (O- or B-star) forms it will heat the gas and remove it from the site of star formation (through winds, ionising radiation, or supernovae). The removal of a (very significant) fraction of the (gas) mass in a region will have a (very significant) effect on the potential felt by the stars that remain. If the stars are unbound or very loosely bound at formation they will be dispersed, and gas expulsion merely speeds this process somewhat. However, if the stars are bound then gas expulsion can completely destroy the cluster, or leave a bound core which will be seen as a naked cluster. It must happen that bound cores are left after gas expulsion as many old, bound clusters are seen (most strikingly, globular clusters).

A key question to address is what can be said about the initial conditions of old, bound clusters? What must be true is that they have survived gas expulsion and therefore they must have been bound at the onset of gas expulsion.

Most previous work on gas expulsion has concentrated on clusters that are in virial and dynamical equilibrium at the onset of gas expulsion (see e.g. Tutukov 1978; Hills 1980; Goodwin & Bastian 2006; Baumgardt & Kroupa 2007). In such a situation the primary factor controlling the survival of

a cluster is the true SFE, secondary factors are the timescale of gas expulsion (adiabatic gas expulsion is less destructive), and the tidal radius (expansion over the tidal radius can rapidly destroy a cluster), as shown in detail by Baumgardt & Kroupa (2007).

However, observations of star formation lead us to believe that stars do not form in equilibrium. They certainly seem to form in a complex distribution that follows the gas (e.g. Larson 1995; Testi et al. 2000; Cartwright & Whitworth 2004; Gutermuth et al. 2005; Allen et al. 2007; Kirk et al. 2007; Schmeja et al. 2008; Gutermuth et al. 2009; Peretto & Fuller 2009; Bressert et al. 2010; di Francesco et al. 2010; Maury et al. 2011), they seem to form with a lower velocity dispersion than the gas (André 2002; Walsh et al. 2004; Adams et al. 2006; Peretto et al. 2006; Kirk et al. 2007; Proszkow & Adams 2009), and their early evolution appears to be dramatic (e.g. Bastian et al. 2008; Allison et al. 2009; Allison et al. 2010).

In this paper we have shown that if the initial *stellar* distribution is out-of-equilibrium then the effect of gas expulsion can be very stochastic (see also Smith et al. 2011a,b). In particular, there are several key factors:

1. The effective SFE (measured by us as the LSF): the relative stellar and gas masses at the onset of gas expulsion (see also Verschueren & David 1989; Goodwin 2009). The higher the effective SFE, the greater the survivability.
2. The stellar virial ratio (Q_{ge}): the virial state of the *stars* alone at the onset of gas expulsion. The lower the stellar virial ratio, the greater the survivability.
3. The time of the onset of gas expulsion: this effects to what extent the stars and gas can relax and/or decouple and so changes the effective SFE and stellar virial ratio. From our simulations, the earlier the onset of gas expulsion the greater the stochasticity in survivability.
4. The timescale of gas expulsion: instantaneous gas expulsion is more destructive than adiabatic (see also Baumgardt & Kroupa 2007).
5. Tidal radius: whilst we have not simulated this, there is no reason to think it should not have the same effect as that found by Baumgardt & Kroupa 2007.

The first four of these factors are all stochastic and depend on the details of the initial conditions.

We reiterate here that our initial conditions are not realistic. We evolve equal-mass stars in a static background potential which we then remove in a simplistic way. However, we find it impossible to see how more realism could possibly produce *less* stochasticity. Indeed, more realistic initial conditions should introduce vast quantities of variables that are potentially important.

For example, a realistic clumpy, live gas potential could react in very different ways. Depending on the details of the gas it could couple well to the stars (i.e. lower the LSF by moving with the stars), or couple badly (by being accreted or removed from subclumps, e.g. Kruijssen et al. 2012). Depending on the structure of the gas, feedback could be less efficient, possibly escaping through bubbles (e.g. Dale & Bonnell 2011), changing the onset of significant gas expulsion and/or its timescale. In addition, realistic small- N subclumps would contain a mass spectrum of stars, include binaries, and have a wealth of possible N -body interactions

that are extremely stochastic on their own (Allison et al. 2010).

In summary, there is no reason to think that if one cluster survives and another does not that they had very different initial conditions. Two sets of *statistically* identical initial conditions can produce a cluster that retains most of its stars or one that is completely destroyed. The final outcome depends on a wealth of different variables (only a handful of which we have rather simplistically modelled here), as well as the details of the initial conditions.

5 SUMMARY & CONCLUSIONS

We perform N -body simulations of sub-structured, non-equilibrium $2500M_{\odot}$ clusters with $500M_{\odot}$ of stars in $N = 1000$ equal-mass particles. A static background potential provides a gas mass of $2000M_{\odot}$ surrounding the stars. The initial true star formation efficiency is fixed at 20 per cent. Gas expulsion is modelled as a reduction in the mass of the background potential over time. We allow the instant that gas expulsion begins, and the duration over which gas expulsion occurs, to vary.

We use two parameters to characterise the state of the cluster at the moment of gas expulsion. The Local Stellar Fraction (LSF) is a measure of the relative contribution of gas and stars to the potential felt by the stars. The stellar virial ratio is a measure of how relaxed the stellar component is.

Our key results may be summarised as follows.

(i) In initially clumpy, and non-equilibrium clusters, a slower rate of gas loss increases the survival of the cluster (in keeping with previous results).

(ii) If gas is expelled within an initial crossing time the effect of gas expulsion is completely stochastic and there are no good global indicators of its effects.

(iii) If gas is expelled after a few crossing times then a combination of the LSF (or rather the efficiency of the coupling of the gas to the stars), and stellar virial ratio are required to parameterise cluster survival, although it is still rather stochastic.

(iv) If gas is expelled after several crossing times the stellar component is generally relaxed and the LSF alone is a good indicator of the effects of gas expulsion. However, the LSF can substantially differ from the true star formation efficiency due to the decoupling of the gas and stars.

Our simulations have been very simple numerical experiments. However we feel they do capture some important physics.

Firstly, the coupling of the stars and gas is crucial to the survival of a cluster. If the stars are able to relax to a more concentrated distribution than the gas (or conversely, if the gas is able to expand relative to the stars), then the dramatic effects of gas expulsion are reduced.

Stochasticity is important: the exact level of decoupling from the gas, and the details of the stellar phase space distribution are also crucial. Gas expulsion whilst the stars are still ‘clumpy’ can completely destroy one cluster, whilst leaving another – statistically identical – cluster with most of its stars in a bound cluster. This depends on the bulk virial ratio of the stars, and also the details of the clump velocities. It is

only after several initial crossing times – after a cluster has relaxed into a rough equilibrium – that stochasticity reduces in importance. However even at this point, stochasticity in the earlier evolution can still influence the final equilibrium configuration.

We would argue that more realistic initial conditions and physics (e.g. a mass spectrum of stars, a clumpy live gas potential, feedback, etc.) can only work to make the problem *more* stochastic, rather than less. Therefore we contend that it is impossible to give a ‘standard’ outcome for any statistically identical clusters: some will be destroyed, while others will survive with different mass and structure. For this reason it is impossible to go backwards from an observed surviving cluster to its initial conditions except in a very broad statistical sense. Therefore we urge caution in deriving the initial cluster population from an observed naked cluster population.

ACKNOWLEDGEMENTS

MF was acknowledges support through FONDECYT grant 1095092, RS was financed through a combination of FONDECYT grant 3120135 and a COMITE MIXTO grant, and PA was financed through a CONCICYT PhD Scholarship.

REFERENCES

- Aarseth S. J., 2003, Gravitational N-Body Simulations
 Adams F. C., Proszkow E. M., Fatuzzo M., Myers P. C., 2006, *ApJ*, 641, 504
 Allen L., Megeath S. T., Gutermuth R., Myers P. C., Wolk S., Adams F. C., Muzerolle J., Young E., Pipher J. L., 2007, in Reipurth B., Jewitt D., Keil K., eds, *Protostars and Planets V The Structure and Evolution of Young Stellar Clusters*. pp 361–376
 Allison R. J., Goodwin S. P., Parker R. J., de Grijs R., Portegies Zwart S. F., Kouwenhoven M. B. N., 2009, *ApJL*, 700, L99
 Allison R. J., Goodwin S. P., Parker R. J., Portegies Zwart S. F., de Grijs R., 2010, *MNRAS*, 407, 1098
 André P., 2002, *Ap&SS*, 281, 51
 Bastian N., Gieles M., Goodwin S. P., Tranco G., Smith L. J., Konstantopoulos I., Efremov Y., 2008, *ArXiv e-prints*, 806
 Bate M. R., 2009, *MNRAS*, 397, 232
 Bate M. R., Bonnell I. A., 2004, in Lamers H. J. G. L. M., Smith L. J., Nota A., eds, *The Formation and Evolution of Massive Young Star Clusters Vol. 322 of Astronomical Society of the Pacific Conference Series, Computer Simulations of Star Cluster Formation via Turbulent Fragmentation*. p. 289
 Baumgardt H., Kroupa P., 2007, *MNRAS*, 380, 1589
 Baumgardt H., Kroupa P., Parmentier G., 2008, *MNRAS*, 384, 1231
 Bonnell I. A., Bate M. R., Vine S. G., 2003, *MNRAS*, 343, 413
 Bressert E., Bastian N., Gutermuth R., Megeath S. T., Allen L., Evans II N. J., Rebull L. M., Hatchell J., John-

- stone D., Bourke T. L., Cieza L. A., Harvey P. M., Merin B., Ray T. P., Tothill N. F. H., 2010, *MNRAS*, 409, L54
- Cartwright A., Whitworth A. P., 2004, *MNRAS*, 348, 589
- Dale J. E., Bonnell I., 2011, *MNRAS*, 414, 321
- di Francesco J., Sadavoy S., Motte F., Schneider N., Henemann M., Csengeri T., Bontemps S., Balog Z., et al., 2010, *A&A*, 518, L91
- Gieles M., Portegies Zwart S. F., 2011, *MNRAS*, 410, L6
- Girichidis P., Federrath C., Banerjee R., Klessen R. S., 2011, *MNRAS*, 413, 2741
- Goodwin S. P., 2009, *Ap&SS*, 324, 259
- Goodwin S. P., Bastian N., 2006, *MNRAS*, 373, 752
- Gutermuth R. A., Megeath S. T., Myers P. C., Allen L. E., Pipher J. L., Fazio G. G., 2009, *ApJS*, 184, 18
- Gutermuth R. A., Megeath S. T., Pipher J. L., Williams J. P., Allen L. E., Myers P. C., Raines S. N., 2005, *ApJ*, 632, 397
- Hills J. G., 1980, *ApJ*, 235, 986
- Kirk H., Johnstone D., Tafalla M., 2007, *ApJ*, 668, 1042
- Kroupa P., Boily C. M., 2002, *MNRAS*, 336, 1188
- Kruijssen J. M. D., Maschberger T., Moeckel N., Clarke C. J., Bastian N., Bonnell I. A., 2012, *MNRAS*, 419, 841
- Lada C. J., 2010, *Royal Society of London Philosophical Transactions Series A*, 368, 713
- Lada C. J., Lada E. A., 2003, *ARA&A*, 41, 57
- Larson R. B., 1995, *MNRAS*, 272, 213
- Maury A. J., André P., Men'shchikov A., Könyves V., Bontemps S., 2011, *A&A*, 535, A77
- Parmentier G., Gilmore G., 2007, *MNRAS*, 377, 352
- Parmentier G., Goodwin S. P., Kroupa P., Baumgardt H., 2008, *ApJ*, 678, 347
- Peretto N., André P., Belloche A., 2006, *A&A*, 445, 979
- Peretto N., Fuller G. A., 2009, *A&A*, 505, 405
- Proszkow E., Adams F. C., 2009, *ApJS*, 185, 486
- Schmeja S., Kumar M. S. N., Ferreira B., 2008, *MNRAS*, 389, 1209
- Testi L., Sargent A. I., Olmi L., Onello J. S., 2000, *ApJL*, 540, L53
- Tutukov A. V., 1978, *A&A*, 70, 57
- Verschueren W., David M., 1989, *A&A*, 219, 105
- Walsh A. J., Myers P. C., Burton M. G., 2004, *ApJ*, 614, 194